

Electronic Supplementary Information (ESI)

A Sheet-like Tin-based Metal-organic Framework with Enhanced lithium Storage

Zikang Ruan^{a#}, Tingting Jiang^{a#}, Xianhe Meng^{a*}, Xiaoyu Hu^c, Qiaoling Kang^a, Lijing Yan^a,
Nengjun Yu^{a,b}, Bingyu Liu^b, Meiqiang Fan^a, Tingli Ma^a

^a College of Materials and Chemistry, China Jiliang University, Hangzhou, 310018, China.

^b Mianyang Liangda Technology Innovation and Service Co., Ltd., Mianyang, 621050, China.

^c State Key Laboratory of Silicon and Advanced Semiconductor Materials, Key Laboratory of Advanced Materials and Applications for Batteries of Zhejiang Province, School of Materials Science and Engineering, Zhejiang University, Hangzhou, 310027, China.

E-mail: mengxhe@cjlu.edu.cn (X. Meng)

1. Experimental details

1.1 Materials

2,5-Dichloroterephthalic acid (C₈H₄Cl₂O₄, 97%) was purchased from Shanghai Aladdin Biochemical Technology Co. Stannous sulfate (SnSO₄, 99%), sodium hydroxide (NaOH, 96%) were purchased from Shanghai McLean Biochemical Technology Co. Acetylene black conductive agent, Super P Li conductive agent was purchased from TIMCAL (Switzerland). Button cell case (CR2025), copper foil, and nickel foam were purchased from Guangdong Candlelight New Energy Technology Co. Diaphragm (Celgard 2400) was purchased from CELGARD, USA. Lithium metal wafers were purchased from Tianjin Zhongneng Lithium Co. The electrolyte (LiPF₆ in EC: DEC=1:1V/V) was purchased from Suzhou Duoduo Chemical Technology Co. Polyvinylidene fluoride (PVDF, HSV900) was purchased from ARKEMA, France. All reagents do not require further purification.

1.2 Synthesis of Sn-DCTP by hydrothermal process

Sn-DCTP was prepared by a simple hydrothermal method. 10mmol of 2,5-dichloroterephthalic acid and 10mmol of sodium hydroxide were dissolved in 30 mL of deionized water (denoted as solution A), and 5mmol of tin sulfate was dissolved in 20mL of deionized water (denoted as solution B). Solution B was poured into solution A and stirred with a glass rod for 1 min to obtain a milky white mixture. The mixture was transferred to a 100 mL PTFE-lined stainless steel reactor, reacted at 170 °C for 72 h, and cooled to room temperature at a rate of 10 °Ch⁻¹. The resulting precipitate was collected, washed by centrifugation with deionized water 5 times, and dried under vacuum at 100 °C for 12h to obtain a yellow-white Sn-DCTP powder.

1.3 Materials characterization

The samples were analyzed by XRD using a Bruker AXS D8 Advance and a Rigaku SmartLab X-ray diffractometer. The diffractometer used Cu K α rays with a scanning range of $2\theta = 3-90^\circ$, a scanning step of 0.02° , and a scanning speed of $5^\circ/\text{min}$. A field emission scanning electron microscope (FESEM) of the type Zeiss Sigma 300 and Hitachi SU8010 with an accompanying EDS was used for the microscopic observation of the samples and elemental analysis. Samples with weak electrical conductivity were sprayed with gold before testing. A JEOL JEM 2100F transmission electron microscope with an accelerating voltage of 200 kV and a resolution of 0.24 nm was used to observe the microforms and lattice fringes of the samples, and an X-ray photoelectron spectrometer (XPS) of Thermo Scientific K-Alpha was used to analyze the surface elements of the samples. Nitrogen adsorption and desorption tests were performed using Micromeritics ASAP 2460 and Micromeritics TriStar II 3020 specific surface area and porosity analyzers. For microporous samples, the Langmuir model was used to calculate the specific surface area, and the HK (Horvath-Kawazoe) model was used to calculate the pore size distribution.

1.4 Electrochemical Measurements

The active substance (i.e., sample), conductive additive (Super P Li or acetylene black), and binder (polyvinylidene fluoride, PVDF) were first mixed and ground in a

mortar and pestle for half an hour at a certain mass ratio, where Sn-DCTP: Super P Li: PVDF = 7:2:1. The mixture was transferred to a small glass vial, and the appropriate amount of N-methyl pyrrolidone (NMP) was added dropwise. The mixture was magnetically stirred for 5 hours to form a slurry of suitable consistency. The slurry was uniformly coated onto a flat copper foil using an applicator. The coated pole piece was first dried at 60 °C for 1 hour and then at 100 °C for 12 hours under vacuum. Finally, the electrode is cut into 14 mm diameter rounds and pressed at 8 MPa. The button cell was assembled in a high-purity argon glove box (Etelux Lab 2000 model, water-oxygen content is less than 0.01 ppm) in the order of positive shell, electrode sheet, diaphragm, lithium sheet, nickel foam, and negative shell from the top down, and the electrolyte was added dropwise with sufficient amount of electrolyte. The positive and negative shells were CR2025, the counter electrode was a 15.6 mm diameter lithium metal wafer, the diaphragm was a 19 mm diameter polypropylene (PP), and the electrolyte was a 1 mol L⁻¹ mixture of LiPF₆ dissolved in a 1:1 volume ratio of ethylene carbonate (EC) and diethyl carbonate (DEC). The assembled batteries were tightly sealed using a hydraulic encapsulator. Before testing. The batteries were allowed to stand for 24 hours to reach a relatively stable state.

Cyclic voltammetry and electrochemical impedance tests were performed using a CHI 660E electrochemical workstation. The cyclic voltammetry tests were performed over a voltage range of 0.01-3 V at a scan rate of 0.2 mV s⁻¹, and the electrochemical impedance tests were performed over a frequency range of 100 kHz-0.01 Hz, and the Nyquist plots were fitted with ZView software. The constant-current cyclic charge/discharge and multiplication performance tests were performed using a LAND CT3001A battery test system, and the batteries were placed in a constant temperature chamber at 30 °C. The voltage range of the test was 0.01-3 V. The battery was tested in a constant temperature oven at 30 °C. The GITT testing was performed using the NEWARE battery testing system with a 30 min constant current charge and a 60 min rest.

2. Additional Supporting Data

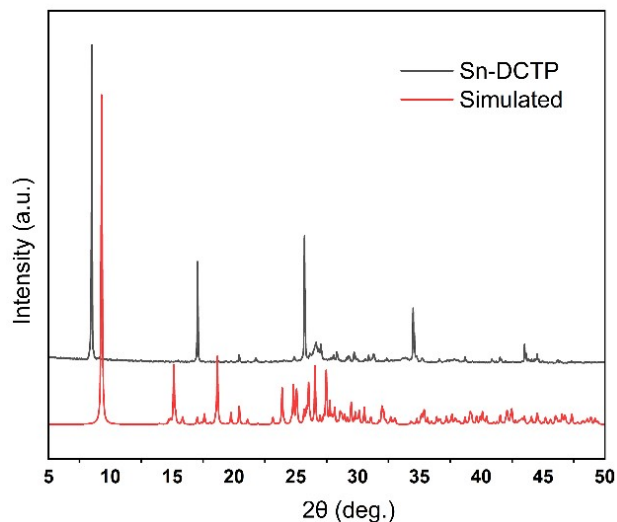


Fig.S1. The XRD patterns of Sn-DCTP.

The simulated XRD pattern is provided according to the X-ray structure of Sn(II)-BDC.¹

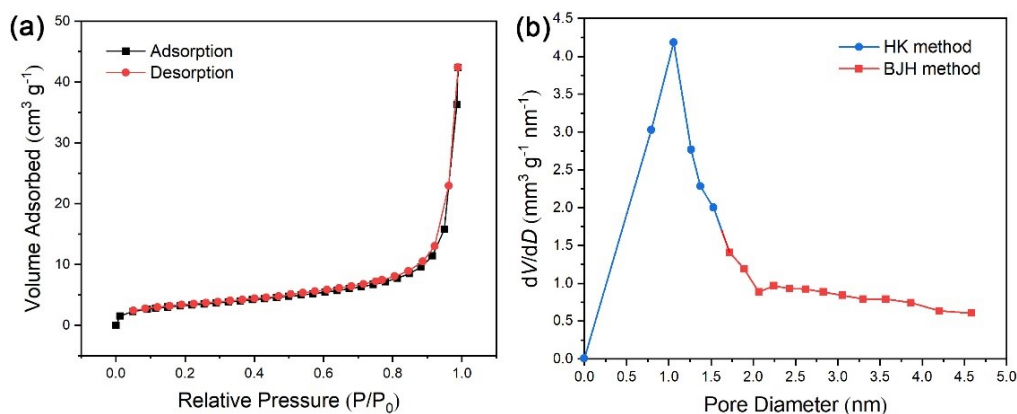


Fig.S2. (a) Nitrogen adsorption-desorption isotherms and (b) pore size distributions of Sn-DCTP.

As shown in Fig. S2a, the nitrogen adsorption and desorption isotherms of Sn-DCTP are of type II. The pore size distribution in the microporous and mesoporous ranges was calculated using the HK (Horvath-Kawazoe) model and the BJH (Barrett-Joyner-Halenda) model, respectively. The results, as shown in Fig. S2b, indicate that Sn-DCTP is dominated by 0-2 nm micropores, with the center of the pore size distribution being about 1 nm, and that there is a certain homogeneous distribution in the mesoporous range, which is probably related to the stacking of the crystal particles.

The Langmuir model calculates that the specific surface area of Sn-DCTP is $107.4 \text{ m}^2\text{g}^{-1}$. The porous structure of Sn-DCTP can promote the penetration of electrolytes, and the high specific surface area can provide abundant lithium storage sites.

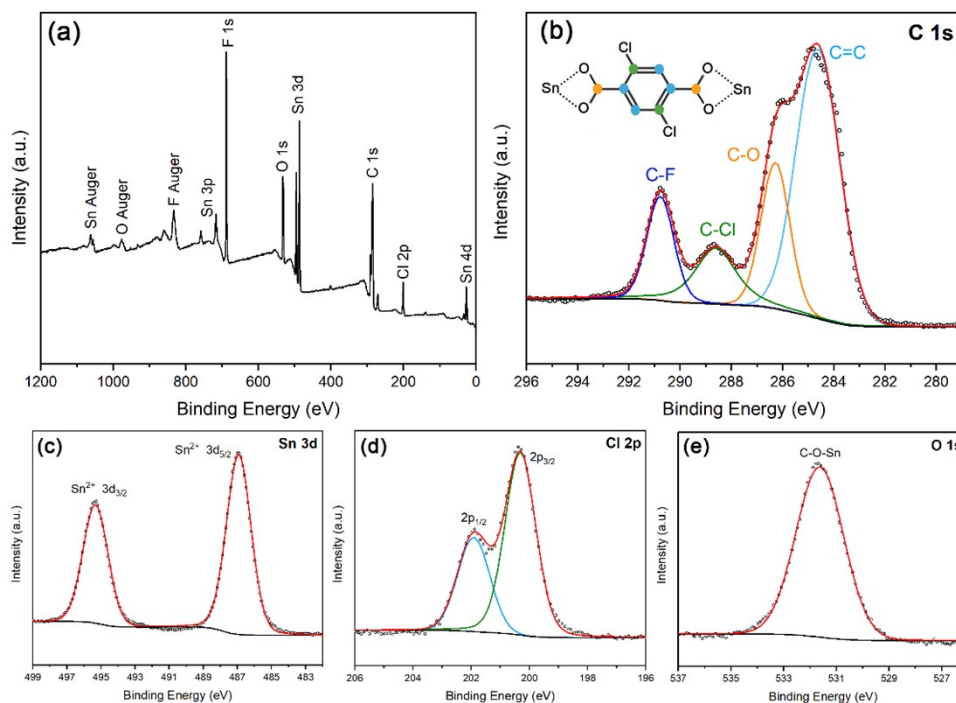


Fig.S3. XPS spectra of Sn-DCTP electrode: (a) wide scan survey spectrum; (b-e) high-resolution spectra for C 1s, Sn 3d, Cl 2p, and O 1s.

Fig. S3a shows a wide scanning range survey spectrum, which detects the elements C, Sn, Cl, and O from Sn-DCTP and F from the polyvinylidene fluoride binder. Fig. S3b shows the fine spectrum of the C 1s orbital, which can be divided into four peaks: the peak located at 284.6 eV corresponds to the four carbons on the benzene ring that are not bonded to Cl (as shown by the blue dots in the small Fig.); the peak located at 286.3 eV corresponds to the carbons of the C-O bond (orange dots in the small Fig.); and the peak located at 288.6 eV corresponds to the C -Cl bonds (green dots in the small Fig.); the peak at 290.8 eV corresponds to the carbon atoms of the C-F bonds of polyvinylidene fluoride. Fig. S3c shows the fine spectrum of the Sn 3d orbital, which can be divided into two peaks, $3d_{3/2}$ (495.3 eV) and $3d_{5/2}$ (486.9 eV), and corresponds to the Sn^{2+} valence state, indicating that it forms a coordination bond with O. Fig. S3d shows the fine spectrum of the Cl 2p orbital, which can be divided into two peaks, $2p_{1/2}$ (201.9 eV) and $2p_{3/2}$ (200.3 eV), and corresponds to the chlorine atoms that form the

C-Cl bond. Fig. S3e shows the fine spectrum of the O 1s orbital, located at 531.6 eV, which corresponds to the oxygen atom forming the C-O-Sn bond. In addition, it is noted that the peak shape of O 1s is wider, probably coupled by two unequal O-Sn bonds.

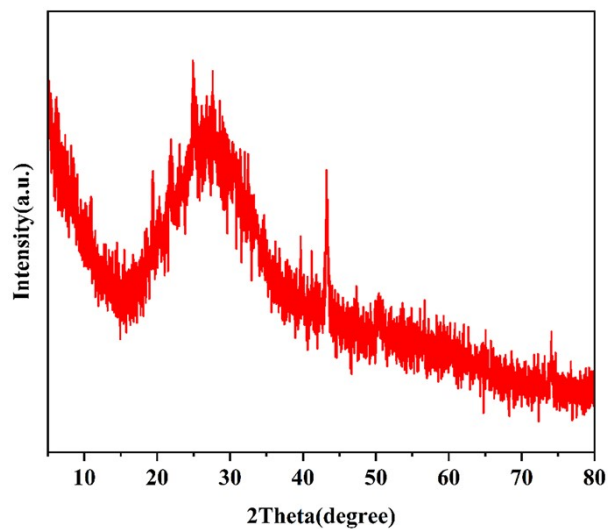


Fig.S4. XRD pattern of the Sn-MOF anode after charge-discharge 1000 times at 800 mA g^{-1} ($2\theta \sim 43^\circ$ corresponds to the (111) face characteristic peak of the copper current collector).

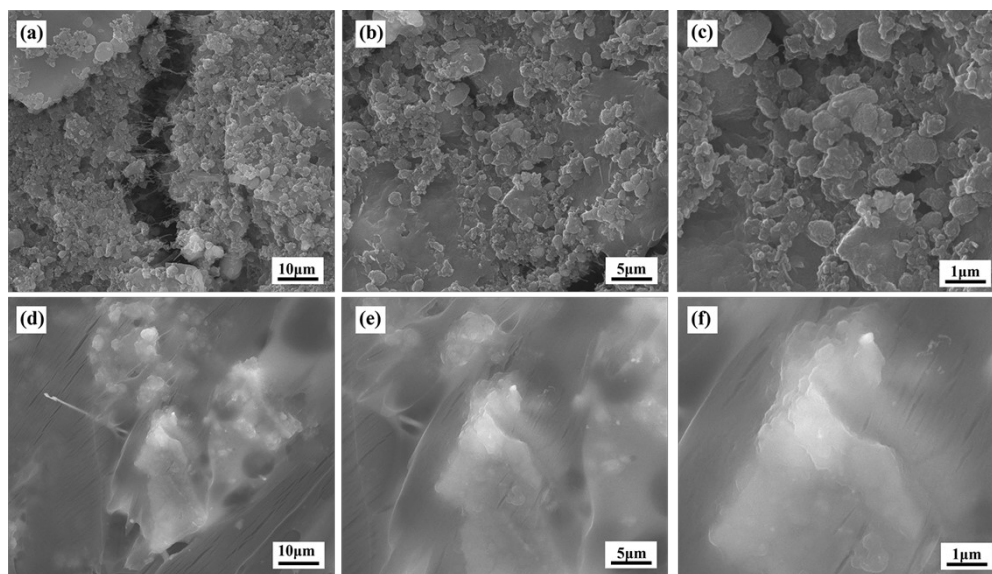


Fig.S5. SEM images of the electrode (a-c) images before cycling, (d-f) Images after after cycling 1000 times at 800 mA g^{-1} .

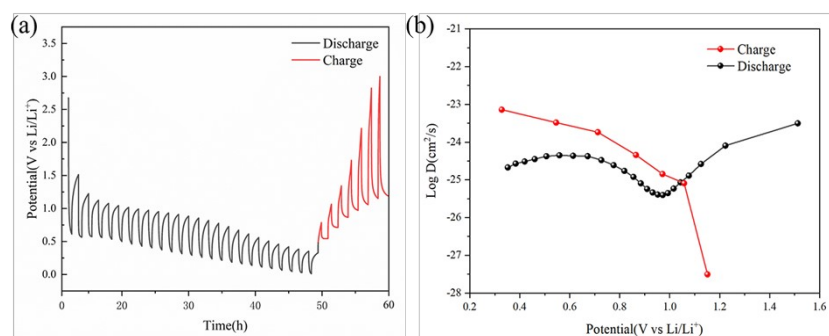


Fig.S6. (a) GITT test of the electrode after cycling 1000 times at 800 mA g^{-1} , (b) Lithium diffusion coefficient.

Table S1 Comparison of Sn-MOFs anode materials.

Sn-MOFs	Organic ligand	Initial library Len efficiency	Cycling performance (specific capacity/ current density/cycles)	literature
Sn-DCTP	2,5-Dichloroterephthalic acid	51.8%	$1021.6 \text{ mAh g}^{-1}/0.2 \text{ A g}^{-1}/100$	This Article
Sn-1,4-BDC	Terephthalic acid	44.2%	$561 \text{ mAh g}^{-1}/20 \text{ mA g}^{-1}/200$	Ref. ²
Sn-1,2-BDC	Phthalic acid	—	$\sim 650 \text{ mAh g}^{-1}/0.2 \text{ A g}^{-1}/250$	Ref. ³
Na-Sn-BDC	Terephthalic acid	53.4%	$523 \text{ mAh g}^{-1}/15 \text{ mA g}^{-1}/5$	Ref. ⁴
Sn-PMA	1,2,4,5-Benzenetetracarboxylic acid	42.2%	$541.3 \text{ mAh g}^{-1}/0.2 \text{ A g}^{-1}/100$	Ref. ⁵
Sn-Httc	Trithiocyanuric acid	43.8%	$945 \text{ mAh g}^{-1}/0.2 \text{ A g}^{-1}/100$	Ref. ⁶
Sn ₂ (dobdc)	2,5-dihydroxyterephthalic acid	53.0%	$731 \text{ mAh g}^{-1}/0.2 \text{ A g}^{-1}/200$	Ref. ⁷
Sn ₂ (dobpdc)	4,4'-Dihydroxybiphenyl-3,3'-dicarboxylic acid	49.5%	$1018 \text{ mAh g}^{-1}/0.2 \text{ A g}^{-1}/200$	Ref. ⁷

Table S1 summarizes the currently reported anode materials for Sn-MOFs, which shows that Sn-DCTP has the highest lithium storage capacity. It is noted that although

Sn₂(dobpdc) also has a high specific capacity, its ligand preparation is complicated and its price is much higher than that of H₂DCTP. Therefore, Sn-DCTP is a competitive and promising anode material for Sn-MOFs.

References

1. X. Wang, L. Liu, T. Makarenko and A. J. Jacobson, *Crystal Growth & Design*, 2010, **10**, 3752-3756.
2. N. Wu, W. Wang, L.-Q. Kou, X. Zhang, Y.-R. Shi, T.-H. Li, F. Li, J.-M. Zhou and Y. Wei, *Chemistry – A European Journal*, 2018, **24**, 6330-6333.
3. X. Zhou, Y. Yu, J. Yang, H. Wang, M. Jia and J. Tang, *ChemElectroChem*, 2019, **6**, 2056-2063.
4. N. Wu, Y.-J. Yang, T. Jia, T.-H. Li, F. Li and Z. Wang, *Journal of Materials Science*, 2020, **55**, 6030-6036.
5. S.-B. Xia, L.-F. Yao, H. Guo, X. Shen, J.-M. Liu, F.-X. Cheng and J.-J. Liu, *Journal of Power Sources*, 2019, **440**, 227162.
6. Y. Kamakura, S. Fujisawa, K. Takahashi, H. Toshima, Y. Nakatani, H. Yoshikawa, A. Saeki, K. Ogasawara and D. Tanaka, *Inorganic Chemistry*, 2021, **60**, 12691-12695.
7. J. Liu, D. Xie, X. Xu, L. Jiang, R. Si, W. Shi and P. Cheng, *Nature Communications*, 2021, **12**, 3131.